

Measurement Concept for a Possible Clearance of Mercury Waste from Nuclear Facilities – 19138

Larissa Klač*, Philipp Ritz*, Marius Hirsch**, Andreas Havenith**, John Kettler**, Andreas Wilden*,
Natalia Daniels*, Giuseppe Modolo*

* Forschungszentrum Jülich GmbH, 52428 Jülich, Germany, +49 2461 616282

** Aachen Institute for Nuclear Training GmbH, Cockerillstrasse 100 (DLZ), 52222 Stolberg (Rhld.),
Germany, +49 2402 127505 5111

ABSTRACT

This paper describes the development of a measurement concept for a clearance of mercury waste from the decommissioning of nuclear facilities. A decontamination of mercury is performed after which large parts of the waste could possibly be released into reuse or conventional mercury disposal. The focus of this work is on the development and validation of a gamma-spectrometric measurement setup that is used for decision-making measurements for a possible clearance procedure. The measurement system is validated by a comparison of experimental measurements with nuclear simulations using *Monte Carlo N-Particle*®^a Transport Code (*MCNP*®). The validated *MCNP*® simulation model is used to determine the energy-dependent photopeak efficiencies and subsequently the sensitivity of the measurements. Preliminary results of gamma spectrometry in combination with *MCNP*® simulations indicate that a clearance of elemental mercury should be possible after decontamination.

INTRODUCTION

The decommissioning of nuclear facilities is accompanied by the accumulation of special problematic nuclear waste for which no standard disposal concepts apply. Such waste includes irradiated nuclear graphite and activated / contaminated toxic metals like beryllium or mercury. [1-2] For example, about 600 kg of radioactively contaminated mercury, used as sealing material in hot cell facilities, have been accumulated in Jülich. [3] More mercury-containing waste is expected to arise in Germany and other countries from the decommissioning of spallation sources and early experimental fast reactors, where mercury was used as target and cooling material, respectively. [1] Next to the complex radionuclide inventory, handling and disposal of mercury and mercury compounds is challenging due to the high chemical toxicity and mobility of most mercury compounds in the environment.

A disposal concept for radioactively contaminated mercury waste is currently developed in the PROMETEUS project (“**PRO**cess of radioactive **ME**rcury **T**reatment under **EU** Safety-standards”), a joint federal German research project between Forschungszentrum Jülich GmbH and Aachen Institute for Nuclear Training GmbH, funded by the German Federal Ministry of Education and Research (BMBF). [3-4] This project aims at the characterization and decontamination of existing waste to release the majority of the mercury into reuse or conventional mercury disposal and thus minimize the amount of mercury that needs to be disposed of in a repository for nuclear waste. A clearance procedure is developed for this purpose comprising a gamma-spectrometric measurement setup for decision-making measurements. The measurements must confirm that the activity inventory is below allowed clearance values [5-8]. Further treatment options are developed for the residues that remain after the decontamination process, including their conversion into a solid material as well as possible immobilization processes.

The first important step when aiming at the disposal of radioactively contaminated mercury waste is a full radiological characterization.

^a *MCNP*® and *Monte Carlo N-Particle*® are registered trademarks owned by Los Alamos National Security, LLC, manager and operator of Los Alamos National Laboratory.

The main challenges in the characterization and clearance of mercury are caused by the high density of mercury (13.5 kg/L), that leads to a high intrinsic shielding of radiation, and by the inhomogeneity of the contaminations in the mercury waste. A concept for the radiological characterization was developed in the course of this project including a gamma-spectrometric measurement setup to reduce the effects of shielding and to detect and analyze an inhomogeneous activity distribution in the mercury samples. [4]

Analyses of several mercury waste quotas from Jülich have shown that the radioactive contaminations are mainly floating on top of the mercury in form of inhomogeneous oils, sludge and/or solid particles. The radioactive contamination is mainly comprised of Cs-137+ and Sr-90+, with lower activities of different actinides (Am-241, Cm-244, Pu-239/240) and Eu-154. A mechanical separation already leads to a significant decontamination of the elemental mercury. Further purification can be achieved by vacuum distillation or washing of mercury. [1] Therefore, large parts of the mercury should be suitable for a release into reuse or conventional mercury disposal.

To achieve a clearance of decontaminated mercury samples, a conservative activity determination is mandatory. For this purpose, *MCNP*® simulations of the gamma detector setup are performed taking into account the geometry and efficiency of the detectors and the geometry and composition of the sample. [5-6] The photopeak efficiencies and detection limits are thus determined by considering the density of mercury and thus including shielding effects that are caused by the mercury matrix. With the help of the *MCNP*® simulations, the measurement setup was analyzed and optimized to evaluate if the setup is sensitive enough to measure key nuclides of the nuclide vector, mainly Cs-137+. Only if the sensitivity is high enough, the measurement setup can be used for decision-making measurements for clearance. [5-8]

This work gives an overview of the aims and challenges of decision-making measurements for a possible clearance of mercury waste from nuclear facilities and presents the experimental procedure and the most important results. The design and the evaluation of the developed gamma-spectrometric measurement facility specialized for clearance measurements of mercury waste samples as well as the results from the *MCNP*® simulation studies will be presented in detail.

DESCRIPTION OF THE GAMMA DETECTOR SETUP AND *MCNP*® SIMULATION

The basis of this work is a gamma-spectrometric measurement setup consisting of two coaxial semi-planar p-type High Purity Germanium (HPGe) detectors obtained from ORTEC®, AMETEK® GmbH, Meerbusch, Germany. The detectors are positioned on a linear slide guide facing each other with a variable distance in between (Fig. 1) to measure thin, geometry-optimized mercury samples simultaneously from opposite sides to increase the sensitivity of the measurements.



Fig. 1. Left: 2 HPGe detectors with a relative efficiency of 25% (left detector) and 22% (right detector) positioned on a slide guide. Right: Final gamma detector setup including lead shielding.

The challenge in the gamma-spectrometric measurement of mercury samples is an adequate efficiency calibration as the samples are inhomogeneous and have a high intrinsic shielding. An experimental efficiency calibration is not possible for an unknown activity distribution in inhomogeneous mercury samples. An *MCNP*® simulation study was therefore conducted to find the most conservative parameters for an activity determination in a clearance procedure. The aim of the *MCNP*® simulations was to provide an adequate calculation of the photopeak efficiency at the most conservative point, which is the point of the lowest photopeak efficiency inside the sample, ensuring that the activity calculated with the help of the *MCNP*® model is always higher than the actual activity in the sample.

The detector setup was modeled with *MCNP*® 6.2 according to the detector specifications as provided by the manufacturer (Fig. 2). They each consist of a high-purity germanium crystal with an outer Ge/B dead layer surrounded by two aluminum end caps. The differences between both detectors regarding the crystal dimensions were considered (TABLE I).

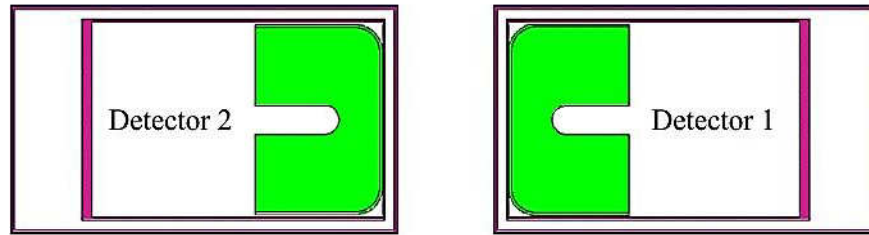


Fig. 2. Detector model created with *MCNP*® 6.2. Left: Detector 2 (ϵ_r 25%). Right: Detector 1 (ϵ_r 22%). Pink: aluminum end cap, green: germanium detector crystal.

Validation of the Detector Model

Different measurements were performed to validate the *MCNP*® detector model with measurements from the detector setup. Different point sources (Am-241: 35.6 kBq, Eu-152: 10.8 kBq, Cs-137+: 21.3 kBq and Co-60: 1.6 kBq at the time of the measurements) were measured at different angles to the detector axis (15° , 30° and 45° , Fig. 3) and distances from the two detectors (5, 10, 20, 25 and 40 cm) and the resulting photopeak efficiencies were compared with the corresponding simulated photopeak efficiencies. The following gamma emission lines were evaluated for the validation of the detector model: 59.54 keV (Am-241); 121.78, 244.70, 344.28, 443.97, 778.90, 867.39, 964.13, 1085.84, 1112.08 and 1408.01 keV (Eu-152); 661.67 keV (Cs-137+), and 1173.23, 1332.49 keV (Co-60). For potential clearance measurements of mercury samples, the activity of the measurements may not be underestimated. Therefore, a simulated photopeak efficiency needs to underestimate the measured photopeak efficiency to maintain this conservative assumption, that means the following condition must be met:

$$\frac{\epsilon(\text{MCNP}^\circ \text{ model})}{\epsilon(\text{measurement})} < 1 \quad (\text{Eq. 1}).$$



Fig. 3. HPGe detector setup including sample holder (red) for validation measurements with point sources at different angles from the detector axis.

The detector model was adapted according to the validation measurements taking into account the necessity for a conservative activity determination of the measurement of mercury samples (adaptions see TABLE I and Fig. 4). The sample is centered between both detectors and the detector models were optimized for a distance of 5 cm between each detector and the middle of the sample ($x = 5$ cm, see Fig. 4) as the clearance measurements will also be performed at that distance. An overview of the adapted detector parameters is presented in TABLE I. For detector 1, the Ge/B dead layer thickness was increased from 0.7 mm to 1.0 mm while the crystal length was decreased from 37.4 mm to 36.0 mm. For detector 2 on the other hand, the dead layer thickness was decreased from 0.7 mm to 0.4 mm while the active detector volume was decreased by decreasing the crystal diameter from 58.5 mm to 56.0 mm. This adapted model is shown in Fig. 4.

TABLE I. Detector parameters of simulated HPGe detectors before the validation (as provided by the manufacturer) and after the validation.

	Detector 2 (ϵ_r 25%)		Detector 1 (ϵ_r 22%)	
	before validation	after validation	before validation	after validation
Crystal diameter (mm)	58.5	56.0	59.0	59.0
Crystal length (mm)	39.6	39.6	37.4	36.0
Dead layer (mm)	0.7	0.4	0.7	1.0

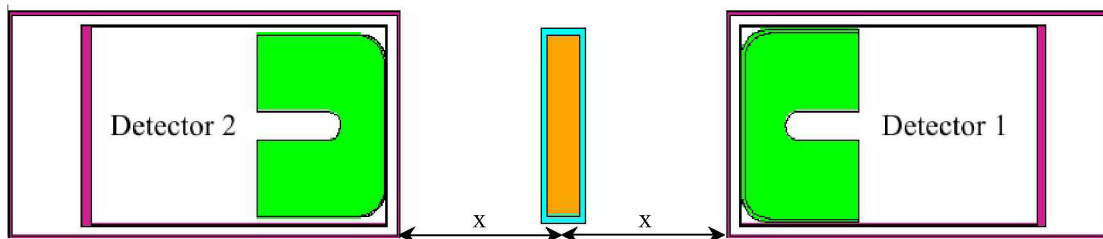


Fig. 4. Validated and adapted detector model with cylindrical sample container created with MCNP® 6.2. Left: Detector 2 (ϵ_r 25%). Right: Detector 1 (ϵ_r 22%). Pink: aluminum end cap, green: germanium detector crystal, turquoise: glass wall of sample container, orange: mercury sample.

Determination of Photopeak Efficiencies

A geometry-optimized sample container was manufactured for measuring mercury samples (Fig. 5). The flask was cylindrical with an inner diameter of 5.56 cm, slightly less than the detector diameter, and a thickness of 1.01 cm to minimize shielding effects due to the high density of mercury (Fig. 4 and Fig. 5). For measurements, this flask is filled with mercury and positioned in the center of the detector axis in the middle between both detectors (Fig. 4 and Fig. 5). A sensitivity analysis was performed to find the point with the lowest photopeak efficiency inside the mercury matrix and determine the corresponding decision threshold and detection limit. Therefore, the flask was modeled with *MCNP*® and simulations were performed with point sources at different positions inside the mercury-filled sample container and the position with the lowest photopeak efficiency was determined and considered for further analysis (Fig. 5). For these simulations, the sum spectrum of both detectors was evaluated as the simultaneous measurement with both detectors leads to an increased sensitivity of the measurements.

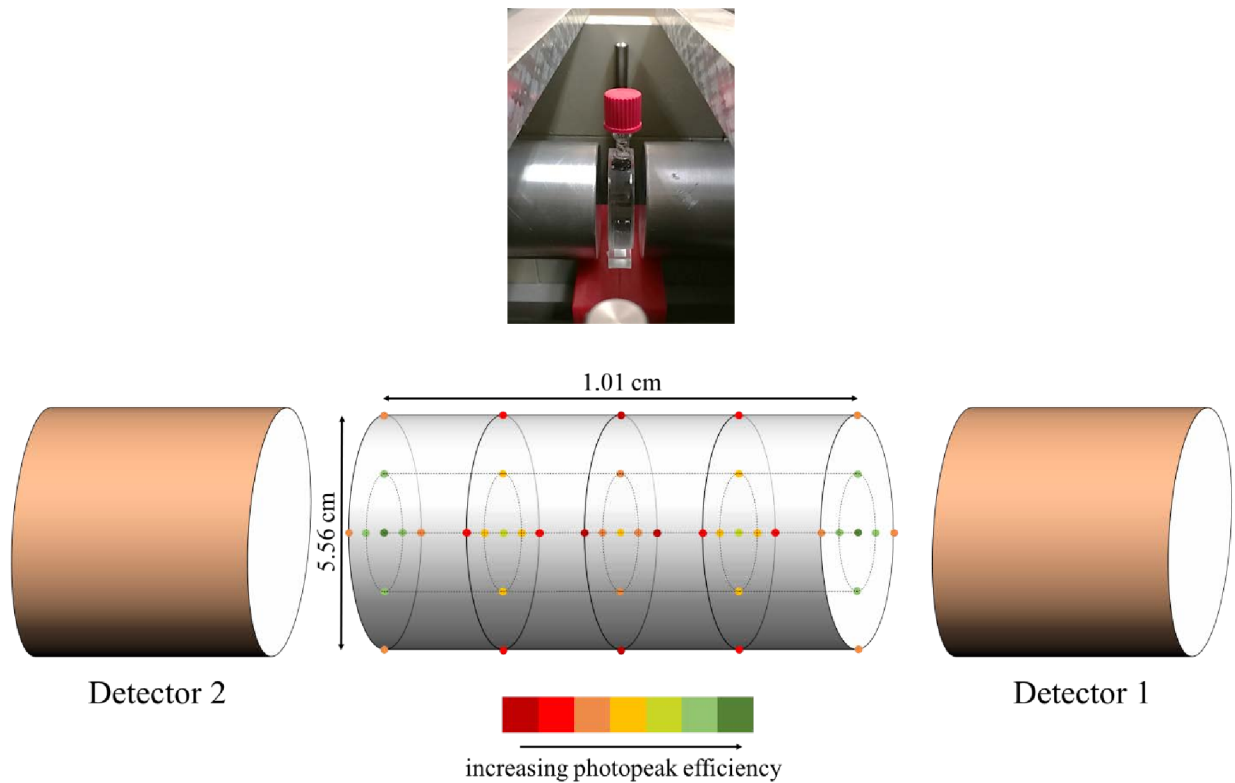


Fig. 5. Top: Cylindrical sample container placed in the HPGc detector setup. Bottom: Distribution of simulated photopeak efficiency for the 661 keV emission line inside the mercury-filled sample container. Dark green: highest photopeak efficiency, dark red: lowest photopeak efficiency.

Fig. 5 shows the cylindrical sample container simulated with *MCNP*® in between both detectors and the different positions in which the point sources (here Cs-137+) were simulated to determine the sensitivity of the measurement procedure. The different colors indicate the variation of the photopeak efficiencies for the 661 keV emission line, emitted by Ba-137m, the daughter nuclide of Cs-137. The lowest photopeak efficiency of $6.07 \cdot 10^{-3} \pm 7.89 \cdot 10^{-6}$ (at a distance between each detector and the middle of the sample of 5 cm) was found in the middle between both detectors, at the outer perimeter of the mercury sample (Fig. 5, dark red spots).

The highest photopeak efficiencies were found in front of each detector in the middle of the cylindrical sample (Fig. 5, dark green spots; photopeak efficiency of 661 keV emission line at a distance between detector and the middle of the sample of 5 cm: $1.02 \cdot 10^{-2} \pm 1.02 \cdot 10^{-5}$ in front of detector 1 and $1.04 \cdot 10^{-2} \pm 1.04 \cdot 10^{-5}$ in front of detector 2).

The simulated efficiency curve for the point with the lowest photopeak efficiency for 661 keV inside a mercury matrix is shown in Fig. 6 (left) and compared to the simulated efficiency curve under the same conditions in air (Fig. 6, right). Without the mercury matrix, the maximum of the photopeak efficiencies is located in the area between the 59 keV emission line of Am-241 and the 244 keV emission line of Eu-152 (Fig. 6, blue circles). For the mercury sample, however, the photopeak efficiency for low energy emission lines, especially at 59 keV (Am-241) and 121 keV (Eu-152), is very low and then rises for higher energy lines due to lower shielding effects at higher emission energies (Fig. 6, red diamonds). Uncertainties range between $\pm 3.68 \cdot 10^{-7}$ and $\pm 7.89 \cdot 10^{-6}$ for the Hg sample and between $\pm 8.11 \cdot 10^{-6}$ and $\pm 1.98 \cdot 10^{-5}$ for the empty sample container; error bars are omitted for clarity. The different trend of the photopeak efficiency for a mercury sample illustrates the shielding effect of the mercury matrix. The efficiency curve for the Hg sample displays a maximum in the region around 600 keV to 800 keV and therefore around the region of the 661 keV emission line. This comparably high photopeak efficiency of the 661 keV emission line is the reason why Cs-137+ was chosen as the reference nuclide in clearance measurements. For the gamma-spectrometric clearance measurements, only the activity of Cs-137+ will be determined directly in each measurement by evaluating the 661 keV emission line. The content of the other nuclides in the sample will then be calculated according to their amounts as determined in the nuclide vector of the mercury samples.

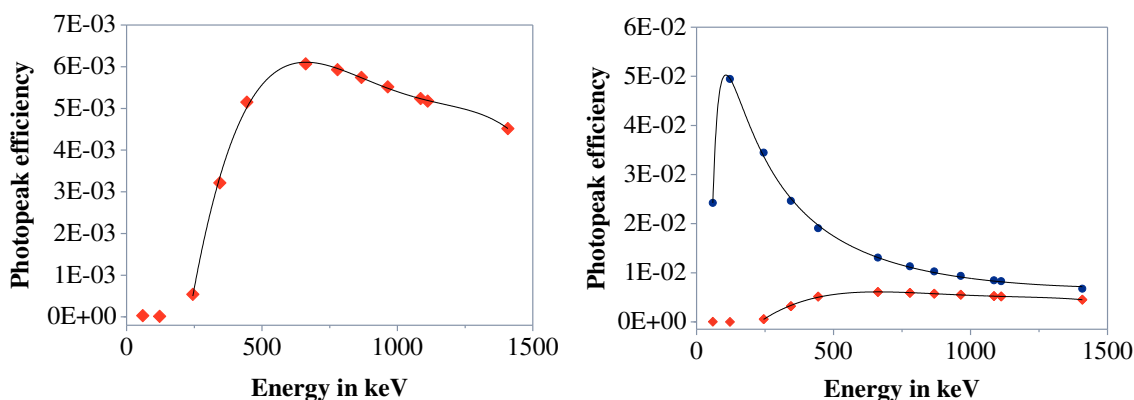


Fig. 6. Simulated photopeak efficiencies (sum spectrum) for a point source at the point of lowest photopeak efficiency for 661 keV inside the cylindrical sample container (sample diameter: 5.56 cm, sample thickness: 1.01 cm) at a 5 cm sample - detector distance. Left: Sample container with simulated Hg matrix. Right: Comparison of Hg matrix (red diamonds) with simulated air matrix (blue circles).

MEASUREMENTS OF MERCURY SAMPLES AND DETERMINATION OF DECISION THRESHOLDS AND DETECTION LIMITS

The cylindrical sample container was filled with a decontaminated mercury sample from the decommissioning of hot cell facilities in Jülich to evaluate the radionuclide content, the quality of decontamination and the possibility of a clearance, i.e. a release into reuse or conventional mercury disposal. The sample was then measured at different positions, i.e. different distances from the detectors, and with different measurement times. The decision thresholds and detection limits for these measurements were calculated according to DIN ISO 11929 to comply with international standards (TABLE II). [9]

The sum spectrum was also used for the determination of decision threshold and detection limit to achieve a higher sensitivity than for a measurement with just one detector. On the other hand, for a decision on the homogeneity of the sample the single spectra can be compared to each other.

TABLE II. Decision threshold and detection limits for the 661 keV emission line determined from the measurement (sum spectrum) for a 324 g Hg sample at different measurement times and distances.

Distance between detector and middle of sample	Measurement time in s	Decision threshold in Bq/g	Detection limit in Bq/g	Determined activity of Cs-137+ in Bq/g
1.275 cm	3600	1.74E-03	3.65E-03	≤ detection limit
1.275 cm	80 000	3.63E-04	7.35E-04	≤ detection limit
1.275 cm	172 800	2.49E-04	5.02E-04	≤ detection limit
5 cm	80 000	3.44E-04	6.96E-04	≤ detection limit

The decision threshold and detection limits are all in the order of 10^{-3} Bq Cs-137+ per gram of sample or lower. Both values can be reduced with longer measurement times. A larger distance between sample and detector should (under constant measurement conditions) normally lead to higher values of decision threshold and detection limit. In the measurements at hand, however, a decrease can be observed when increasing the distance from 1.275 to 5 cm (compare lines 2 and 4 of TABLE II). This can be attributed to the effect of the lead shielding that is increased at higher sample-detector distances (lead bricks are placed below the detectors at higher detector distances), thus reduces the background contribution and therefore the decision threshold and detection limit.

The currently applicable value for an unrestricted clearance of Cs-137+ stated in the German Radiation Protection Ordinance is 0.5 Bq/g Cs-137+ and the value for a clearance for disposal is 10 Bq/g Cs-137+. [7] The clearance value for an unrestricted clearance of Cs-137+ changes with the new German Radiation Protection Ordinance from 0.5 Bq/g to 0.1 Bq/g. [8] The detection limit for a measurement to meet the requirements of such a clearance procedure should be 10% of these clearance values or lower to ensure the applicability of a clearance procedure. The Cs-137+ detection limits for all measurements are well below this 10% criterion even for the most conservative clearance value of 0.1 Bq/g and thus the described measurement setup is suitable for a clearance procedure with an unrestricted clearance of mercury samples.

The activity of Cs-137+ for a real mercury sample was determined from the net peak area of the 661 keV emission line with the most conservative assumptions. In all measurements, this determined activity was below the clearance value for Cs-137+ and would therefore allow an unrestricted clearance of this sample. The activities of the other nuclides listed in the nuclide vector of the mercury samples in Jülich were calculated according to their respective amounts and compared with the respective values for a clearance of each nuclide stated in the Radiation Protection Ordinance as well as the summation formula for clearance. According to these results, a clearance would be possible for all the nuclides that have been determined in the mercury samples.

CONCLUSIONS

This paper presents a possible measurement setup for a clearance procedure of mercury waste from nuclear facilities comprising two HPGe detectors. The detector setup is modeled with *MCNP*® and simulations are performed to determine the photopeak efficiency and the sensitivity of the measurements. The detection limits that are achieved with this measurement setup are below the values required by the German radiation protection ordinance for a release of the mercury waste into reuse or conventional mercury disposal. These results are promising as they prove the possibility of a clearance of mercury waste from nuclear facilities. More measurements of mercury samples will be performed in the near future to evaluate the possibility of a clearance procedure for a larger amount of mercury waste.

REFERENCES

1. INTERNATIONAL ATOMIC ENERGY AGENCY (IAEA), "Management of Problematic Waste and Material Generated During the Decommissioning of Nuclear Facilities", IAEA, Vienna (2006).
2. N. SHCHERBINA, L. KLAß, G. DEISSMANN, D. BOSBACH, "Research for the safe management of nuclear wastes: The special case of "problematic" radioactive waste streams. Energie - Herausforderungen der Energiewende", *Proceedings of "Frühjahrstagung des Arbeitskreises Energie in der Deutschen Physikalischen Gesellschaft"*, Münster, 27-29 March (2017).
3. J. KETTLER, A. HAVENITH, M. HIRSCH, C. GREUL, J. ULRICH, G. MODOLO, A. WILDEN, G. DEISSMANN, L. KLAß, N. LIECK, F. SADOWSKI, "PROcess of Radioactive MERcury Treatment under EU Safety Standards - PROMETEUS", *Proceedings of KONTEC 2017 - 13. Internationales Symposium "Konditionierung radioaktiver Betriebs- und Stilllegungsabfälle"*, Dresden, 22-24 March (2017).
4. L. KLAß, P. RITZ, N. DANIELS, A. WILDEN, G. MODOLO, D. BOSBACH, M. HIRSCH, J. KETTLER, A. HAVENITH, "Characterization Concept for the Disposal of Radioactively Contaminated Mercury Wastes from the Decommissioning of Nuclear Facilities", *Proceedings of 18th Radiochemical Conference*, Mariánské Lázně, 13-18 May (2018).
5. C. J. WERNER (EDITOR), "MCNP Users Manual - code Version 6.2", Los Alamos National Laboratory, report LA-UR-17-29981 (2017).
6. C. J. WERNER, ET AL., "MCNP6.2 Release Notes", Los Alamos National Laboratory, report LA-UR-18-20808 (2018).
7. FEDERAL OFFICE FOR RADIATION PROTECTION (BUNDESAMT FÜR STRAHLENSCHUTZ), "Ordinance on the Protection against Damage and Injuries Caused by Ionizing Radiation (Radiation Protection Ordinance) of 20 July 2001, last amendment of 26 July 2016", Berlin (2016).
8. BUNDESAMT FÜR STRAHLENSCHUTZ, "Verordnung zur weiteren Modernisierung des Strahlenschutzrechts", Berlin (2018).
9. DIN DEUTSCHES INSTITUT FÜR NORMUNG E.V., "DIN ISO 11929: Bestimmung der charakteristischen Grenzen (Erkennungsgrenze, Nachweisgrenze und Grenzen des Vertrauensbereichs) bei Messungen ionisierender Strahlung - Grundlagen und Anwendungen", Berlin (2011).

ACKNOWLEDGEMENTS

Funding for the research project was received from the German Federal Ministry of Education and Research (BMBF) under Grant Agreement numbers 15S9266A–B.